

08.3

## Isotopically purified Si/SiGe epitaxial structures for quantum computing

© D.V. Yurasov<sup>1</sup>, A.V. Novikov<sup>1</sup>, M.V. Shaleev<sup>1</sup>, M.N. Drozdov<sup>1</sup>, E.V. Demidov<sup>1</sup>, A.V. Antonov<sup>1</sup>,  
L.V. Krasilnikova<sup>1</sup>, D.A. Shmyrin<sup>1</sup>, P.A. Yunin<sup>1</sup>, Z.F. Krasilnik<sup>1</sup>, S.V. Sitnikov<sup>2</sup>, D.V. Sheglov<sup>2</sup>

<sup>1</sup> Institute of Physics of Microstructures, Russian Academy of Sciences, Nizhny Novgorod, Russia

<sup>2</sup> Rzhanov Institute of Semiconductor Physics, Russian Academy of Sciences, Siberian Branch, Novosibirsk, Russia

E-mail: Inquisitor@ipmras.ru

Received November 24, 2023

Revised November 24, 2023

Accepted February, 9 2024

In this work, isotopically purified <sup>28</sup>Si/<sup>28</sup>Si<sup>72</sup>Ge heterostructures were fabricated by molecular beam epitaxy. The obtained residual concentration of the <sup>29</sup>Si and <sup>73</sup>Ge isotopes with non-zero nuclear spin was of the order of 1-2 hundred ppm. The maximum electron mobility in the two-dimensional electron gas formed in these structures reached  $\sim 4.5 \cdot 10^4$  cm<sup>2</sup>/(V · s) at  $T = 1.6$  K, which confirms high quality of the fabricated samples. Low concentration of Si and Ge isotopes with non-zero nuclear spin and high crystalline quality allows using such structures in fabricating electron spin qubits.

**Keywords:** SiGe heterostructures, isotopic purification, molecular beam epitaxy, secondary ion mass spectroscopy, spin qubit.

DOI: 10.61011/TPL.2024.05.58424.19813

In view of implementing quantum computations, various physical systems and approaches to the quantum bits (qubits) formation are currently considered: superconducting, based on trapped ions, semiconductor, photonic, etc. [1–3]. Many of them face the problem of scalability due to large size of the qubits. Qubits on semiconductor structures are free of this drawback, since their size could be smaller than a micrometer [4]. The early semiconductor qubits were formed on the GaAs/AlAs heterostructures [5]. However, all qubits based on A<sub>3</sub>B<sub>5</sub> semiconductors have a significant drawback, namely a short time of spin phase coherence, which is caused by non-zero nuclear spin of all isotopes of atoms from III and V groups of the periodic table [6]. This drawback is not inherent to silicon-based qubits since, among the three Si isotopes, only <sup>29</sup>Si has a non-zero nuclear spin. The technique for Si isotopic enrichment and fabrication of <sup>28</sup>Si single crystals with a low content of the <sup>29</sup>Si isotope was developed in the framework of the „Avogadro“ project aimed at creating a mass standard based on the <sup>28</sup>Si-sphere [7]. Another significant advantage of silicon qubits is the possibility of their commercial production based on all the achievements of modern microelectronics [8]. Among various options for implementing Si-based qubits, qubits on Si/SiGe heterostructures may be distinguished, which use the spin of an electron localized in the so-called „electrostatic“ quantum dot (QD) [9,10]. Such a QD is created by a system of surface gates in a strained Si quantum well (QW) confined between the unstrained SiGe barriers. One of the main advantages of the qubit of this type is that its sensitivity to charge noise is lower than that of qubits based on Si MOS (metal-oxide-semiconductor) structures; the main source of the charge noise is charge states in amorphous layers of gate dielectrics [4]. The use of only isotopically purified Si in

forming the Si/SiGe heterostructures is reasonable because the electron is localized in the Si QW and is, therefore, most sensitive to the presence of atoms with non-zero nuclear spin in this very QW. However, Si/SiGe heterostructures have a significant disadvantage of low qubit operation temperature as compared to Si MOS structures due to the small energy separation between the two lowest energy levels (the so-called valley splitting (VS)) [4]. Recently, various approaches have been proposed to enhance VS, including modification of the electron wave function in the Si QW by introducing Ge and SiGe layers into it [11,12]. Thus, in forming the Si/SiGe heterostructures for quantum computing it is important to have a low content of both Si and Ge isotopes with non-zero nuclear spin. This paper reports on formation of Si/SiGe heterostructures by molecular beam epitaxy (MBE) using isotopically purified Si and Ge sources and on studying their structural and transport properties.

The isotopically purified Si/SiGe structures were grown on high-vacuum MBE facility Balzers UMS 500P. In this machine Si and Ge were evaporated from individual electron-beam evaporators (EBEs). For evaporation, we used pieces of isotopically purified <sup>28</sup>Si and <sup>72</sup>Ge single crystals obtained at the G.G. Devyatikh Institute for Chemistry of High-Purity Substances RAS (Nizhny Novgorod). The EBE crucible for silicon evaporation was loaded with pieces of an isotopically purified <sup>28</sup>Si single crystal with an about 100ppm content of the <sup>29</sup>Si isotope with a non-zero nuclear spin. After melting, the pieces of isotopically purified Si were fused into a single volume, and Si evaporation proceeded in the so-called self-crucible mode (Fig. 1,a). In this evaporation mode, Si turns to the liquid state only in the center of the crucible, while crucible walls remain solid (Fig. 1,a). Although Ge has a lower melting point (938°C) than Si (1414°C), its vapor pressure at this

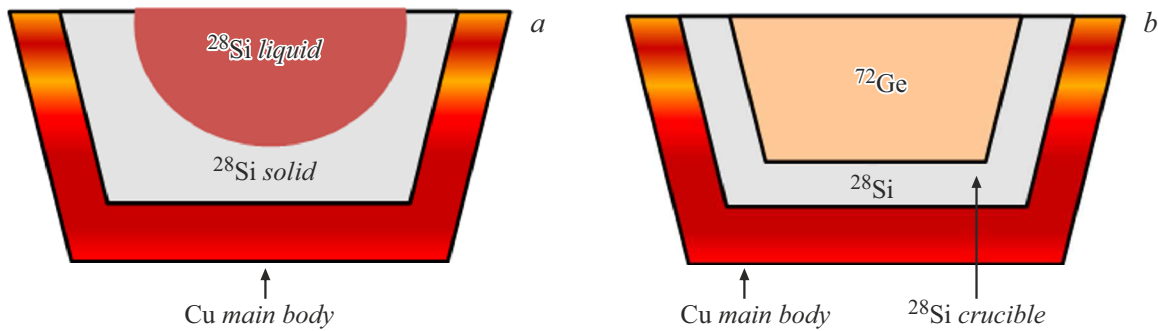


**Figure 1.** *a* — schematic illustration of isotopically purified  $^{28}\text{Si}$  evaporation in the self-crucible mode. *b* — schematic illustration of isotopically purified  $^{72}\text{Ge}$  evaporation from a silicon crucible obtained by the evaporation of a  $^{28}\text{Si}$  portion in the self-crucible mode.

temperature is relatively low [13]. Therefore, to achieve acceptable growth rates, Ge should be heated significantly above its melting point. As a result, Ge loaded into EBE gets melted, and the self-crucible mode does not take place. Contact of liquid Ge with the water-cooled crucible walls makes the Ge evaporation unstable. Previously, it was proposed to solve this problem by using a silicon crucible [14]. This approach was used in this study. To obtain Si/SiGe structures with low content of isotopes with non-zero nuclear spin, a silicon crucible for evaporating isotopically purified  $^{72}\text{Ge}$  was obtained from isotopically purified  $^{28}\text{Si}$ . For this purpose, at the first stage the EBE crucible for evaporating  $^{72}\text{Ge}$  was fully filled with pieces of the  $^{28}\text{Si}$  single crystal. At the second stage, after their melting, a noticeable (up to  $\sim 50\%$ ) portion of  $^{28}\text{Si}$  has been evaporated in the self-crucible mode, which led to formation of a pit. Material remaining after the evaporation of a portion of  $^{28}\text{Si}$  represented the silicon crucible (Fig. 1, *b*). This crucible was loaded with pieces of the isotopically purified  $^{72}\text{Ge}$  single crystal which, formed a single volume of  $^{72}\text{Ge}$  after melting (Fig. 1, *b*). This material was used further for evaporation of  $^{72}\text{Ge}$  during epitaxial growth of the isotopically purified Si/SiGe structures.

Using the system described above, Si/SiGe structures were fabricated; their design is presented in Fig. 2, *a*. The structures were grown on the so-called  $\text{Si}_{1-x}\text{Ge}_x/\text{Si}(001)$  virtual substrates which represent the graded  $\text{Si}_{1-x}\text{Ge}_x$  relaxed buffers with the Ge fraction in the upper layer  $x_{\text{Ge}} \sim 30\%$  (Fig. 2, *a*). The relaxed buffers were obtained from natural sources. The structure grown from isotopically purified sources consisted of an unstrained  $\text{Si}_{1-x}\text{Ge}_x$  layer with  $x_{\text{Ge}} = 30\%$ , and thickness  $h \sim 300$  nm, Si strained QW with  $h \sim 10$  nm, SiGe barrier layer with  $x_{\text{Ge}} = 30\%$  and  $h \sim 45$  nm, and protective Si layer with  $h \sim 2$  nm. The deposition temperature was chosen low enough ( $\sim 500^\circ\text{C}$ ) to avoid relaxation of elastic strains in Si QW and also to obtain sharp Si/SiGe heterointerfaces, which promoted an increase in VS [15]. The absence of elastic strains relaxation in the grown structure was confirmed by X-ray diffraction.

Isotopic composition in the grown structure was studied by using time-of-flight secondary ion mass spectrometer (SIMS) TOF.SIMS-5. According to the SIMS data (with

accounting for isotope calibration as in [16]), the  $^{29}\text{Si}$  content in the grown structure is about 0.01% (Fig. 2, *b*) which corresponds to its concentration of 100 ppm in the initial isotopically purified  $^{28}\text{Si}$  ingot; this is close to the record-low values given in literature [15]. The  $^{73}\text{Ge}$  content in the structure is about 0.02% (Fig. 2, *b*). It is believed that the  $^{73}\text{Ge}$  content in the grown structure is higher than that in the evaporating material ( $\sim 100$  ppm in the initial  $^{72}\text{Ge}$ -ingot) because of contamination of the Ge EBE crucible with a small amount of naturally purified Ge because the MBE machine was previously used to grow SiGe structures from natural sources. Hence, a small amount of natural material could get into the crucible with isotopically purified Ge from components of the MBE vacuum chamber (from the chamber walls, shutter drives, holders, etc.).

To characterize the transport properties of the obtained Si/SiGe structures, insulated-gate Hall bars were fabricated on them. As the gate dielectric, there was used an  $\text{Al}_2\text{O}_3$  layer with  $h \sim 40$  nm grown by the atomic-layer deposition method. Measurements performed at  $T = 1.6$  K showed that conductivity arose after applying a positive voltage of several volts to a gate. Variation of the gate voltage within a range of several volts (above the threshold) made the sheet electron concentration varying from  $10^{11}$  to  $\sim 10^{12}$   $\text{cm}^{-2}$ . Since a tensile-strained Si QW is a deep potential well for electrons, at low temperatures the structure conductivity is caused by the 2D electron gas transport in it. Based on measuring the Hall effect at  $T = 1.6$  K in the magnetic field of 0.5 T, it was shown that the electron mobility in the 2D electron gas in the above-specified concentration range exceeds  $10^4$   $\text{cm}^2/(\text{V} \cdot \text{s})$ ; the maximum of  $\sim 4.5 \cdot 10^4$   $\text{cm}^2/(\text{V} \cdot \text{s})$  was observed at electron concentrations of  $\sim (8.5-9) \cdot 10^{11}$   $\text{cm}^{-2}$ . The obtained mobility values are high enough to allow such structures to be used for qubit fabrication [15].

Thus, in this work the isotopically purified Si/SiGe heterostructures with a low (of about several hundred ppm) concentrations of both Si and Ge isotopes with non-zero nuclear were fabricated by MBE. High quality of the obtained structures has been confirmed by measuring their low temperature transport properties. Low content of  $^{29}\text{Si}$  and  $^{73}\text{Ge}$  isotopes with non-zero nuclear spin in the

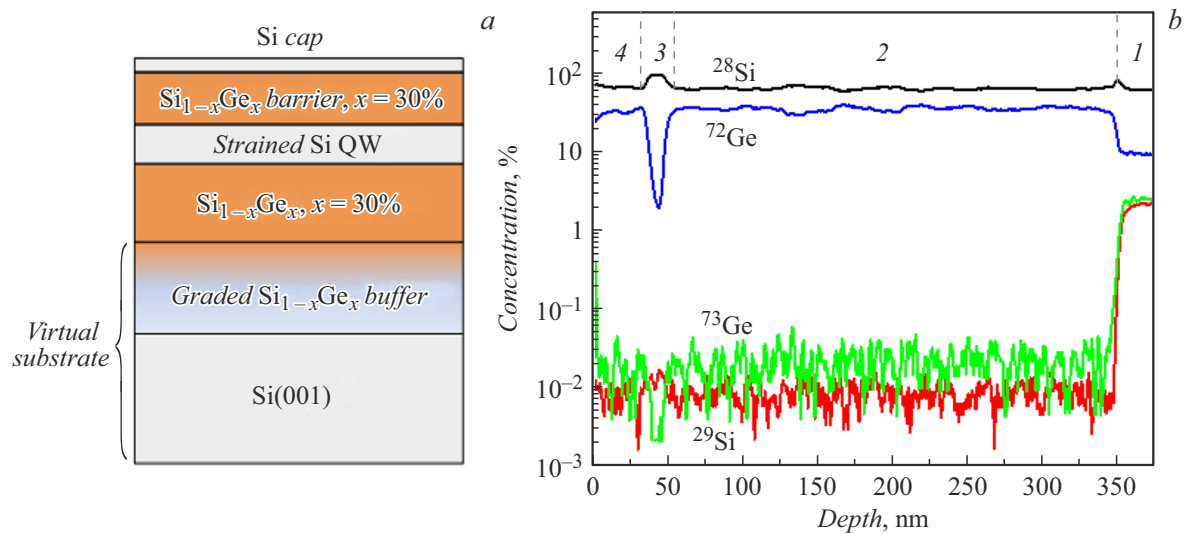


**Figure 2.** *a* — schematic representation of the grown structure. *Virtual substrate* — substrate used in the study which is based on relaxed buffer  $\text{Si}_{1-x}\text{Ge}_x/\text{Si}(001)$  ( $x \sim 30\%$ ) obtained from natural sources. *b* — atomic distributions of different Si and Ge isotopes in the grown Si/SiGe structure obtained from SIMS. In the figure, digits indicate — the region of the relaxed SiGe buffer obtained from natural sources (1), unstrained SiGe buffer (2), Si QW (3), and SiGe barrier layer (4). Layers 2–4 were grown using isotopically purified sources.

obtained structures, as well as their high quality, makes it possible to apply them for further fabrication of electron spin qubits.

### Funding

The work on growing and studying isotopically purified SiGe heterostructures was supported by Rosatom within the framework of Quantum Computing „Roadmap“ (contract № 868-1.3-15/15-2021 of 10/5/2021 and contract № P2194 of 12/14/2021); the work was performed by using the equipment of Common Use Center „Physics and Technology of Micro— and Nanostructures“ of IPM RAS.

### Conflict of interests

The authors declare that they have no conflict of interests.

### References

- [1] N.P. de Leon, K.M. Itoh, D. Kim, K.K. Mehta, T.E. Northup, H. Paik, B.S. Palmer, N. Samarth, S. Sangtawesin, D.W. Steuerman, *Science*, **372**, eabb282 (2021). DOI: 10.1126/science.abb2823
- [2] Y. Kim, A. Eddins, S. Anand, K.X. Wei, E. van den Berg, S. Rosenblatt, H. Nayfeh, Y. Wu, M. Zaletel, K. Temme, A. Kandala, *Nature*, **618**, 500 (2023). DOI: 10.1038/s41586-023-06096-3
- [3] C.D. Bruzewicz, J. Chiaverini, R. McConnell, J.M. Sage, *Appl. Phys. Rev.*, **6**, 021314 (2019). DOI: 10.1063/1.5088164
- [4] G. Burkard, Th.D. Ladd, A. Pan, J.M. Nichol, J.R. Petta, *Rev. Mod. Phys.*, **95**, 025003 (2023). DOI: 10.1103/RevModPhys.95.025003
- [5] J.R. Petta, A.C. Johnson, J.M. Taylor, E.A. Laird, A. Yacoby, M.D. Lukin, C.M. Marcus, M.P. Hanson, A.C. Gossard, *Science*, **309**, 2180 (2005). DOI: 10.1126/science.1116955
- [6] P. Stano, D. Loss, *Nat. Rev. Phys.*, **4**, 672 (2022). DOI: 10.1038/s42254-022-00484-w
- [7] K. Fujii, H. Bettin, P. Becker, E. Massa, O. Rienitz, A. Pramann, A. Nicolaus, N. Kuramoto, I. Busch, M. Borys, *Metrologia*, **53**, A19 (2016). DOI: 10.1088/0026-1394/53/5/A19
- [8] A.M.J. Zwerver, T. Krähenmann, T.F. Watson, L. Lampert, H.C. George, R. Pillarisetty, S.A. Bojarski, P. Amin, S.V. Amitonov, J.M. Boter, R. Caudillo, D. Correas-Serrano, J.P. Dehollain, G. Droulers, E.M. Henry, R. Kotlyar, M. Lodari, F. Lüthi, D.J. Michalak, B.K. Mueller, S. Neyens, J. Roberts, N. Samkharadze, G. Zheng, O.K. Zietz, G. Scappucci, M. Veldhorst, L.M.K. Vandersypen, J.S. Clarke, *Nat. Electron.*, **5**, 184 (2022). DOI: 10.1038/s41928-022-00727-9
- [9] A. Noiri, K. Takeda, T. Nakajima, T. Kobayashi, A. Sammak, G. Scappucci, S. Tarucha, *Nature*, **601**, 338 (2022). DOI: 10.1038/s41586-021-04182-y
- [10] X. Xue, M. Russ, N. Samkharadze, B. Undseth, A. Sammak, G. Scappucci, L.M.K. Vandersypen, *Nature*, **601**, 343 (2022). DOI: 10.1038/s41586-021-04273-w
- [11] T. McJunkin, B. Harpt, Y. Feng, M.P. Losert, R. Rahman, J.P. Dodson, M.A. Wolfe, D.E. Savage, M.G. Lagally, S.N. Coppersmith, M. Friesen, R. Joynt, M.A. Eriksson, *Nat. Commun.*, **13**, 7777 (2022). DOI: 10.1038/s41467-022-35510-z
- [12] M. Friesen, P. Rugheimer, D.E. Savage, M.G. Lagally, D.W. van der Weide, R. Joynt, M.A. Eriksson, *Phys. Rev. B*, **67**, 121301(R) (2023). DOI: 10.1103/PhysRevB.67.121301
- [13] <https://www.mbe-komponenten.de/selection-guide/vapor-pressure.php>

- [14] V.V. Postnikov, A.V. Novikov, *Sposob vyrashchivaniya kremniy-germanievyykh geterostruktur*, patent RF № 2407103 (20.12.2010). (in Russian)  
<https://www.fips.ru/iiss/document.xhtml?faces-redirect=true&id=6a0ddea4abe978a8af3a9f1472e560f5>
- [15] A. Hollmann, T. Struck, V. Langrock, A. Schmidbauer, F. Schauer, T. Leonhardt, K. Sawano, H. Riemann, N.V. Abrosimov, D. Bougeard, L.R. Schreiber, *Phys. Rev. Appl.*, **13**, 034068 (2020).  
DOI: 10.1103/PhysRevApplied.13.034068
- [16] M.N. Drozdov, Yu.N. Drozdov, A.V. Novikov, P.A. Yunin, D.V. Yurasov, *Semiconductors*, **48**, 1109 (2014).  
DOI: 10.1134/S1063782614080090.

*Translated by EgoTranslating*